Open Access

SCHOLARENA

Journal of Material Science and Metallurgy

RESEARCH ARTICLE

Effect of Carbon Black Loading on Linear Low-Density Polyethylene Properties

Noora Al-Qahtani[1*], Maryam Al-Ejji[1], Mabrouk Ouederni[2], MA AlMaadeed[3] and Nabil Madi[1]

[1]*Center for Advanced Materials, Qatar University, Doha-Qatar*

[2]*Resercher and Development of Qatar Petrochemical Company, QAPCO, Doha-Qatar*

[3]*Vice President for Research and Graduate, Qatar University, Doha-Qatar*

[*]**Corresponding author:** Noora Alqahtani, Center for Advanced Materials, Qatar University, PO Box: 2713, Doha-Qatar, Tel: +97444033977, E-mail: noora.alqahtani@qu.edu.qa

Citation: Noora Al-Qahtani, Maryam Al-Ejji, Mabrouk Ouederni, MA AlMaadeed, Nabil Madi (2021) Effect of Carbon Black Loading on Linear Low-Density Polyethylene Properties. J Mate Sci Metall 2: 102

Abstract

This article studied the mechanical, thermal, electrical, rheology, and morphological properties of low-density polyethylene mixed with carbon black (CB) content of 5%, 10%, and 20% by weight. The optimum mechanical and electrical properties performance was achieved with the addition of 5% carbon black. The drop in properties after adding more CB is due to agglomeration and poor dispersion of carbon particles in the polymer matrix. CB resulted in higher dynamic viscosity and storage modulus at low frequencies, but this phenomenon was reversed at high frequencies. CB resulted in more shear thinning of LLDPE at high shear rates.

Keywords: Carbon Black; Electrical Properties; Thermal Analysis; Rheological Properties

Introduction

Linear low-density polyethylene is a commonly utilized polymer in the industry because of its unique structure and excellent overall performance. It is produced by polymerizing ethylene with a slight amount of an α-olefin. LLDPE, however, is not photodegradation resistant, and its relatively low mechanical properties and thermal stability can sometimes limit its application in industry. The development of particulate reinforced polymer composites is currently viewed as one of the highly promising methodologies in the area of next-generation engineering products [1–3]. Polymer composites are an essential category of polymers that has broad applications in a number of various industrial areas and therefore have been comprehensively researched in the last few decades [4–7]. Inorganic fillers are believed to be extremely critical both technologically and economically, including carbon black, which is very valuable in the thermoplastic industry [8]. Further, the development of electrical conductivity in low carbon black content [9] enhances mechanical and thermal properties of particular concern. The high feature percentage in mixture with high particle porosity, high strength, and compatibility with organic materials constituted carbon black, a potential candidate as support for polymeric materials. Effective development of the carbon black properties in polymers is consequently associated to their homogeneous dispersion in the matrix. The carbon black dispersion is strongly dependent on carbon black content, and therefore a percolation threshold value for the composite should be investigated. Carbon black used as fillers in many polymers such as ultra-high molecular weight polyethylene (UHMWPE) [10,11], high density polyethylene (HDPE) [12,13], ethylene butylacrylate copolymer (EBA) [14], ethylene–octene elastomer (EO) [15], low molecular weight polyethylene (LMWPE) [16], Low-density

polyethylene (LDPE) [17] and Polypropylene (PP) [17]. The fillers were around 0.5wt% to 5wt%. Many authors have investigated the addition of CB to LLDPE due to its low cost and conductive properties [18–20] [18-21]. Pin Zhouet *et al.* [18] experiment with the electrical properties of the CB-filled LLDPE/EMA composites and higher percolation threshold due to the good interaction between EMA and CB. The stability of CB-filled LLPE is important and studded by V.M Goldberg *et al.* [18] for thermo oxidative degree, and artificial weathering by M.liu *et al.* [19] both showed that CB has a positive impact on stability. Mechanical properties of CB-filled LLDPE was studied by A.Ahmed *et al.* [21] and showed the electron irradiation important the properties at 250 kGy. This paper discusses the impact of CB on the mechanical, electrical, thermal stability, and rheology of LLDPE. The relation between the microstructure and dispersion of CB is explained.

Most veterinary surgeon remove this tumor by complete incision from epidermis and use electrocutery application to prevent tumor recurrence tumor growth [8]. Other veterinary surgeon or veterinary oncologist are use hormonal therapy, neutering, and chemotherapy [9].

Experimental

Materials

The materials utilized in this research were Linear Low-Density Polyethylene (LLDPE) provided as pellets by Qatar Petrochemical Company (QAPCO) with the following properties, a Melt Flow Index (MFI) of 1.0 g/10 min (190 °C, 2.16 kg) and a density of 0.918 g/cm^3. The average particle size of CB was about 30 nm and a density of 2.5 g/cm^3. The Materials were completely dried before the combination that reduces the impact of moisture [22].

Composite sample preparation

Composite samples were arranged in a two-step process that included compounding and molding. First, LLDPE and CB powders were tumbled mixed in the dry state in the right proportions before being compounded in a Laboratory size FARREL 2 Roll Mill. The mill temperature was set at 160 °C and samples were fed twice into the Mill for a total compounding time of about 12 min. The second step consisted of molding 2 mm thick composite sheets in a Compression Molding Press Machine. The molding cycle consisted of the following: 5 min at a temperature of 180 °C and zero pressure, followed by 5 min at T = 180 °C and P = 1400 psi, and finally about 5 min cooling at a rate of about 15 °C/min. Table 1 indicates the defined symbol for each method and the subsequent compositional ratio of each component.

Designated Symbol	Composition and compositional Ratio (By Weight %)
LLDPE	100 PE/0 CB
PE5CB*	95 PE/5 CB
PE10CB	90 PE/10 CB
PE20CB	80 PE/20 CB

*Abbreviations consist of PE and CB stands for LLDPE and carbon black, respectively

Table 1: Sample's code and their compositions

Differential Scanning Calorimeter (DSC) Measurements

Differential scanning calorimeter assessment was carried out applying a Perkin Elmer Instrument Pyris 6 (DSC) with a sample weight of 5 to 8 mg. All samples were heated at a rate of 10 °C/min to 170 °C, next held for 5 min at 170 °C to remove the earlier thermal history, and then cooled at a rate of 10 °C/min to 30 °C, then held for 5 min at 30 °C and heated again at a rate of 10 °C/min to 170 °C under nitrogen atmosphere (20 ml/min) [22]. The cold crystallization temperature (T_c °C), melting temperature (T_m °C), and heat of fusion were revealed from the second heat scan. The crystallinity of samples (X_c %) was determined employing the subsequent expression [23]:

$$X_c\% = \frac{\Delta H}{\Delta H_f W} \times 100 \quad (1)$$

The crystallinity was determined from the ratio among the melting enthalpy (ΔH) amount from the second scan of the DSC assessment and the melting enthalpy of the 100% crystalline phase (ΔH_f) from the literature [24]. For polyethylene, a ΔH_f value of 289 J/g was utilized [24], and W is the weight fraction of LLDPE in the composites. Half crystallization time ($t_{1/2}$) is the time necessary for 50% of crystallization to be done, which represent the speed of crystallization rate [25], $t_{1/2}$ can be obtained by the following equation [26]:

$$t_{1/2} = \frac{(T_{c.onst} - T_c)}{r} \quad (2)$$

Where (Tc.onst) is the onset temperature of the crystallization process, (Tc) is the crystallization temperature, and (r) is the cooling rate (r).

The crystallinity was determined from the ratio among the melting enthalpy (ΔH) amount from the second scan of the DSC assessment and the melting enthalpy of the 100% crystalline phase (ΔHf) from the literature [24]. For polyethylene, a ΔHf value of 289 J/g was utilized [24], and W is the weight fraction of LLDPE in the composites. Half crystallization time (t1/2) is the time necessary for 50% of crystallization to be done, which represent the speed of crystallization rate [25], t1/2 can be obtained by the following equation [26]:

Thermogravimetric Analysis (TGA) Measurements

Thermogravimetric (TG) and Differential Thermogravimetric (DTG) measurements were performed with Perkin Elmer Pyris Analyzer 6 [22]. The specimens of LLDPE and composites with a weight of about 10 mg were heated from 30 °C to 550 °C at a heating rate of 10 ° C/min [27]. Samples were arranged in a ceramic pan, and the tests were done in a nitrogen atmosphere with N2 being provided at a flow rate of 20 ml/min. In this work, comprehensive and precise aspects identifying the thermal stability based on the temperature at which the sample losses 50% of its weight ($T_{50\%}$) and the temperature of a maximum rate of weight loss (T_{peak}) (from DTG curves) are carried as a measure of thermal stability of the composites [28].

Tensile test Measurements

The composites tensile properties were calculated as per the standard test method ASTM D 638-02 [29]. The composite samples tensile strength was tested by Lloyd instrument's material analysis machine related to a remote microcomputer for data acquisition and evaluation. The load was assessed by a load cell of 50 kN capacity, although the displacement was evaluated by applying an internal extensometer. The speed of examination was 100 mm/min [30]. Samples were examined under a similar requirement for each category of samples. The values described were the average values of three individual amounts [31].

Hardness Test Measurements

A microhardness analysis was organized with all samples by HRF - Rockwell Hardness F Scale by application of load 60 kg, and the provided measurement values were of indentation hardness of a total of 10 indentation points on the sample surface [32]. The slandered was utilized to calculate the hardness of the compounds corresponding to ASTM D785-08.

Morphological Observations

The composite sample microstructures were examined applying a scanning electron microscope (Nova Nano SEM 450) [33]. These samples were fractured in liquid nitrogen into pieces with a surface area of 2mm, each surface of which was coated with a thin layer of gold and then positioned into the SEM. The microstructure of the samples was examined at an accelerating voltage of 3kV. Through the microstructural examination, the interactions among CB and virgin polymer were found [34].

Rheology Characterization

The viscoelastic behavior of the neat polymer and CB reinforced samples were analyzed by melt rheology in an AERS Rheometer. Samples were first molded into 2 mm thick disks, and then rheology measurements were presented to define the storage modulus (G'), loss modulus (G"), and dynamic viscosity (η*). Experiments were finalized over a frequency sweep range among 0.01 and 100 rad/s at a temperature of 210 oC [35].

Electrical Conductivity Measurement

The electrical conductivity was assessed by Kithely 2400 source meter using the two-probe method. The electrical measurement was carried out at room temperature 25 °C. The samples were formulated as disks of 2 mm thickness and covered with a silver sticker on both sides of the disc to ensure good contact of the sample surface with the two aluminum electrodes (1 mm diameter), fixed on the opposite sides of the sample [36]. Figure 1 illustrates the measurement scheme. The specific conductivity σ was measured by means of a device measuring very high resistance. The procedure was set different values of current for measuring the voltage and calculating the resistance (R) [10]. Equation (3) is used to calculate the conductivity where A is the area of discs samples, and L is the length of the disk.

$$\frac{1}{\sigma} = R\frac{A}{L} \tag{3}$$

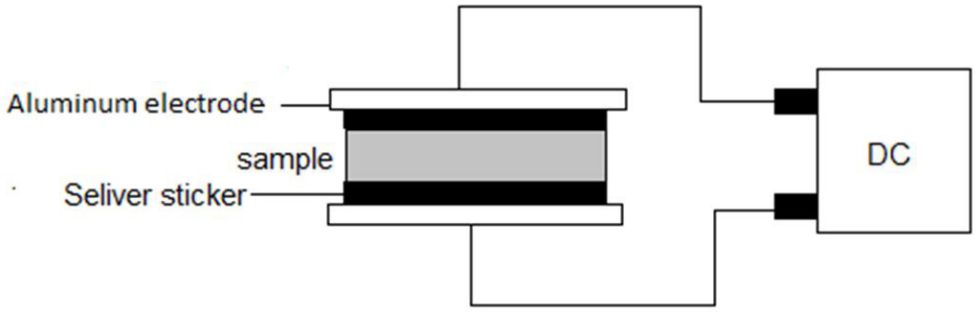

Figure 1: Illustration of the measurement for the electrical conductivity

Results and Discussion

Differential Scanning Calorimeter (DSC) Measurements

Sample ID.	Tm (°C)	Tc (°C)	Xc (%)	$t_{½}$ (min)
LLDPE	122.3	106.1	42.1	0.26
PE5CB	122.3	106.3	42.1	0.3
PE10CB	121.7	106.7	31.1	0.27
PE20CB	122.2	106.3	30.3	0.29

Table 2: Melting Temperature, Crystallization Temperature, % Crystallinity, and half crystallization time of CB composites

The heating and cooling thermograms of the LLDPE/CB composites are shown in Figure 2. The DSC findings in terms of melting point (T_m, °C), crystallization temperature (T_c, °C), and the percentage crystallinity (X_c) are summarized in Table 2. The DSC measurements indicate that variations do not considerably influence composites' melting point in the CB substance. Furthermore, the Xc of composites is not affected by a CB addition of 5 wt.% but then decreased with 10 and 20% of CB addition. A low shoulder might be observed in the low point of temperature side of the melting bend of the LLDPE, indicating paracrystalline structure. A virgin LLDPE has a relatively wide molecular weight distribution and small series branching arrangement. The branches are rather found in the lower molecular weight chains; hence, LLDPE performs as is a combination of higher molecular weight linear and lower molecular weight branched particles [37]. This heterogeneous distribution of polymer chains is considered as a wide melting zone. The CB fragments are recognized to nucleate the polymer crystallization, growing its crystallinity and affecting the nature of the lamella in the crystallite [38]. As can be seen, from Figure 2 and Table 2, the carbon particles' nucleating function in the crystallization of LLDPE is small. At a CB particle of extra than 5 wt.%, the reduction to crystallinity level can be justified by the existence of an extreme amount of CB contents that can obstruct the polymer chain parts' movement and, therefore, prevent crystal growing [28,20]. This can be explained by the fact that crystallization is composed of both nucleation and growth. Even though the CB particles enhance nucleation, growth is significantly reduced due to restrictions on the polymer chains' mobility in

the occurrence of a high concentration of CB particles. The half crystallization time t1/2 was enhanced with the addendum of CB content and generally agreed with the crystallinity results discussed earlier. It can be concluded that the nucleation started, and the crystallization procedure progressed in a relatively short period for the neat polymer [25]. The smaller time of t1/2 represents the faster crystallization rate [39]. The slow crystallization rate of CB composites can be illustrated by the week CB-polymer interactions [40] and slow crystal growth in the presence of CB particles.

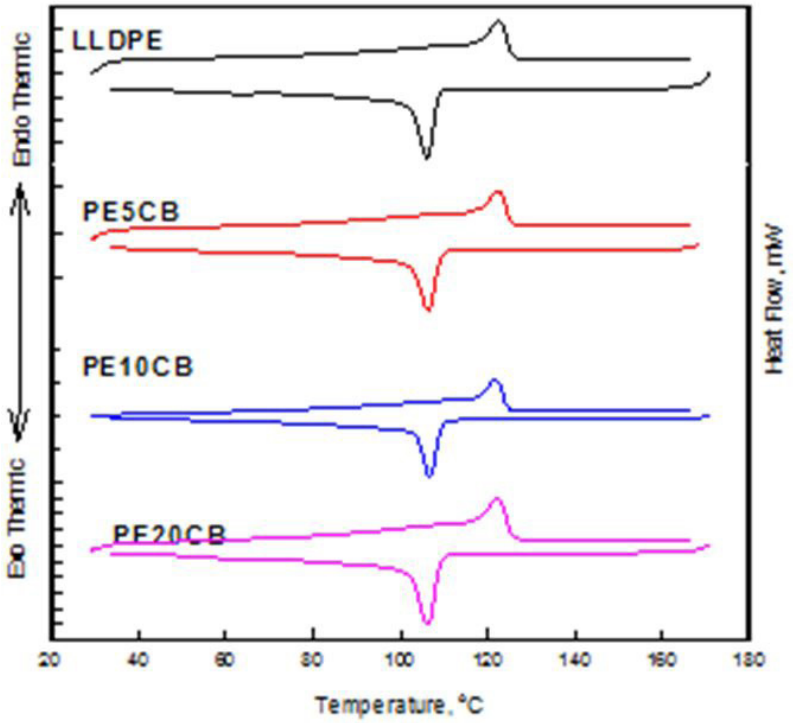

Figure 2: DSC thermo-gram of LLDPE and its composites with carbon black for -melting and cold crystallization profiles

Thermogravimetric Analysis (TGA) Measurements

DTGA curves of pure LLDPE and LLDPE composites with various CB loadings are exhibited in Figure 3. It is viewed that the thermal decomposition of all mixtures happens below 500 °C. The temperature at which a sample drops 50% of its weight ($T_{50\%}$), these were taken from TG curves (not shown), and the temperature of the max rate of weight loss (T_{end}) are carried as an amount of thermal stability of the composites and represented in Table 3. It is apparent from Table 3 that adding CB improves the thermal stability of the composites. The noted growth in thermal stability is believed to be attributable to the limitation of mobility of segmental progress of LLDPE because of the improved interface among the CB and the polymer matrix [40–43].

Sample ID.	Temperature (°C)	
	T50%	Tend
LLDPE	470.1	475.7
PE5CB	472.6	477.4
PE10CB	475.0	479.1
PE20CB	476.3	481.0

Table 3: Change of TGA profiles with different contents in the LLDPE composites

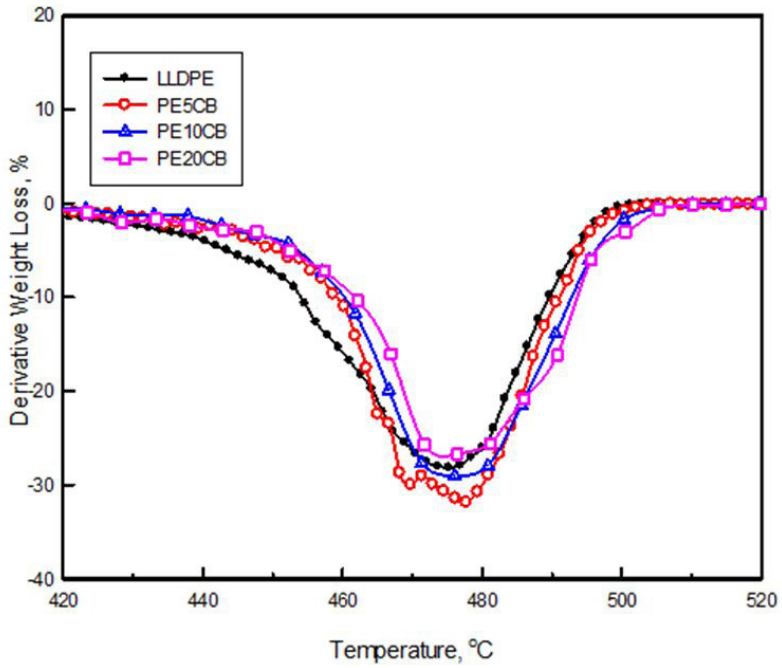

Figure 3: Change of DTGA profiles with varying contents of CB.

Tensile test Measurements

Figure 4 indicates the difference in the tensile strength with the addition of CB. The tensile strength increases significantly by adding CB at 5 wt.%, and then it decreases rapidly when CB content is more than 5 wt.%. This indicates that the optimum carbon black loading in LLDPE is about 5 wt.%. The degree of reinforcement of LLDPE composites increases with filler loading and the extent of polymer-filler interaction. The reduction of tensile strength beyond 5 wt.% loadings can be explained in terms of particle agglomeration at higher CB content [44,45]. These agglomerated, hard particles create concentrated stress points and therefore reduce the stress transfer from polymer chains to carbon particles [20]. So, at higher content, CB particles will exhibit a poor dispersion, and it is evidently challenging to shape strong adhesion, weak surface energy with polymer matrix. This will be shown later in the morphological study.

The influence of CB loading on the modulus of the sample is shown in Figure 5. The neat polymer, LLDPE, is of low tensile modulus 141 MPa; after adding CB, the tensile modulus increases with increasing CB contents, which reveals enhanced stiffness caused by increasing filler substance. A change of distortion performance from ductile to more brittle occurred at higher fillings of CB. As the amount of CB particles increases in the LLDPE matrix, some portions of the polymer are trapped inside the filler network, which increases the effective volume ratio of the solid particles in the composite. On the other hand, the polymer-filler interface might cause the polymer chains' absorption on the filler surface and reduce its progress. Consequently, the polymer viscosity and modulus will be increased [46,47].

From the point of view of packaging technology, agricultural film applications and extension at break are critical factors explaining the ductility of materials below tension. Figure 5 reveals the need for elongation at the break of the mixtures on the CB filling. CB loading of 5 wt.% resulted in elongation at break of PE5CB composite of 1200 %, subsequently its quick reduction with rising CB content. The results indicate that the CB may possibly substantially develop the tensile fracture ductility of LLDPE resin, and the best effect was obtained when CB was 5 wt.%. The filled combinations with polymer matrix breakdown can be introduced through minor defects initiated by stress intensity on the filler surface. Therefore, little cracks are founded, which expand till achieving the vital crack amount. In the identical material without the filler, the creation and expansion of cracks are unintentional, and the collapse appears at reasonably high distortion. The filler findings exist in a more straightforward start of break formation by a stress intensity on the filler surface, and on the one hand, a reduction of chain mobility because of the polymer-filler interface causing lower deformability of the combinations. Both consequences cause a reduction of the elongation at break amounts [45,48].

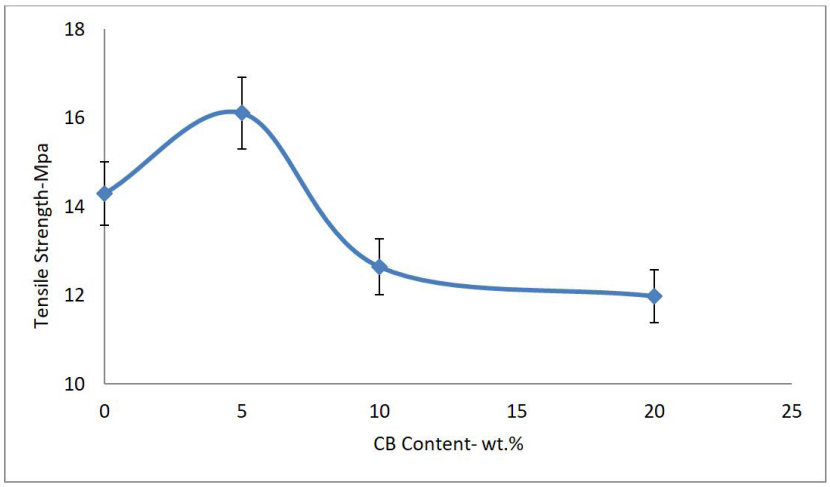

Figure 4: Tensile Strength of CB reinforced LLDPE composites.

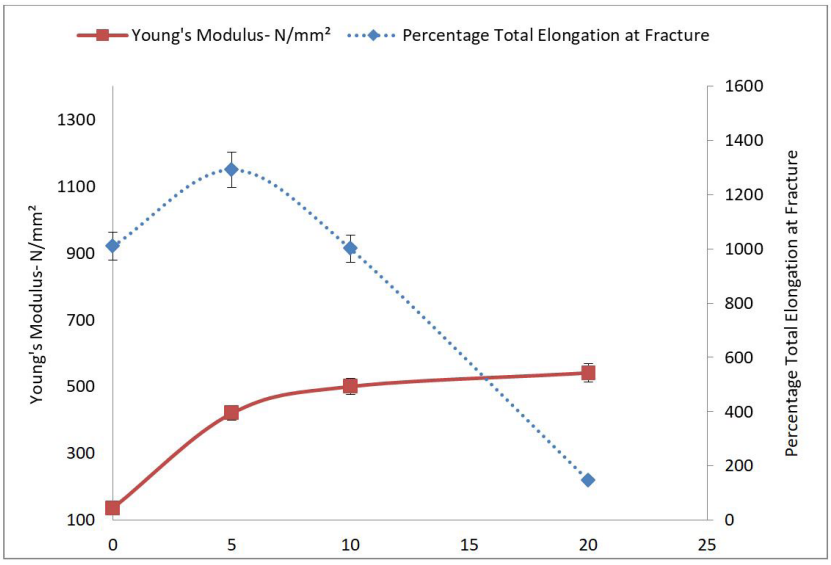

Figure 5: Young's Modulus and Percentage Total Elongation at Fracture for the composites.

Hardness Test Measurements

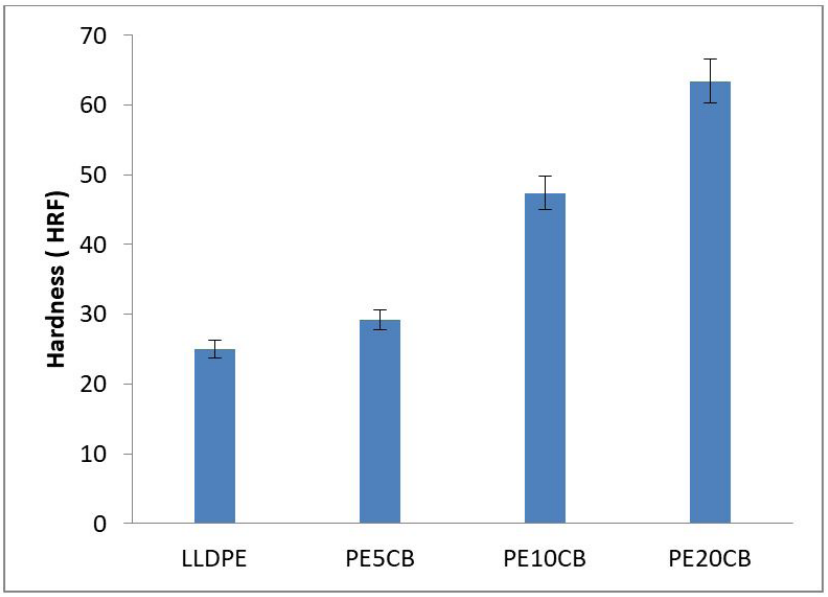

Figure 6: Hardness for LLDPE composites.

Surface hardness is usually examined as one of the extremely vital elements associated with the wear resistance of materials. Figure 6 shows the hardness as a function of CB content in LLDPE. It shows that the hardness of the composite is almost linearly enhanced with rising CB content. This indicates that the addition of CB particles is beneficial for improving the surface hardness of LLDPE composites. CB particles acted as stress concentration points. Therefore, it is expected beyond 5 wt.% of CB content, polymers chains have penetrated into the CB particles agglomerates [49].

Morphological Observations

Figure 7A shows the SEM micrographs of the CB by itself. As shown in the figure, the average size was around 30 nm. Figures 7B-E show the freeze fractured morphology of pure LLDPE and 5,10, and 20 wt.% CB filled LLDPE, respectively. Figures 7C-E show SEM micrographs of agglomerates typically found in these composites. Evidently, as shown in Figure 8 C, 5 wt.% loading, CB particles are distributed in the polymer matrix. As a result, the tensile strength of LLDPE is significantly improved. The used LLDPE has a relatively low melt flow index (MFI = 1.0 g/10 min) and a flow behavior that favors in good dispersion of CB in the polymer matrix, especially at a low CB polymer ratio (lower loading). However, as the CB content rises, CB atoms blend into main aggregates, and Van der Waals forces affect these aggregates to enter in additional loosely assembled agglomerates [20,50], as might be viewed from Figures 7D and E. So, at higher filler loading, one expects a reduction in the tensile strength (c.f. Figure 4)

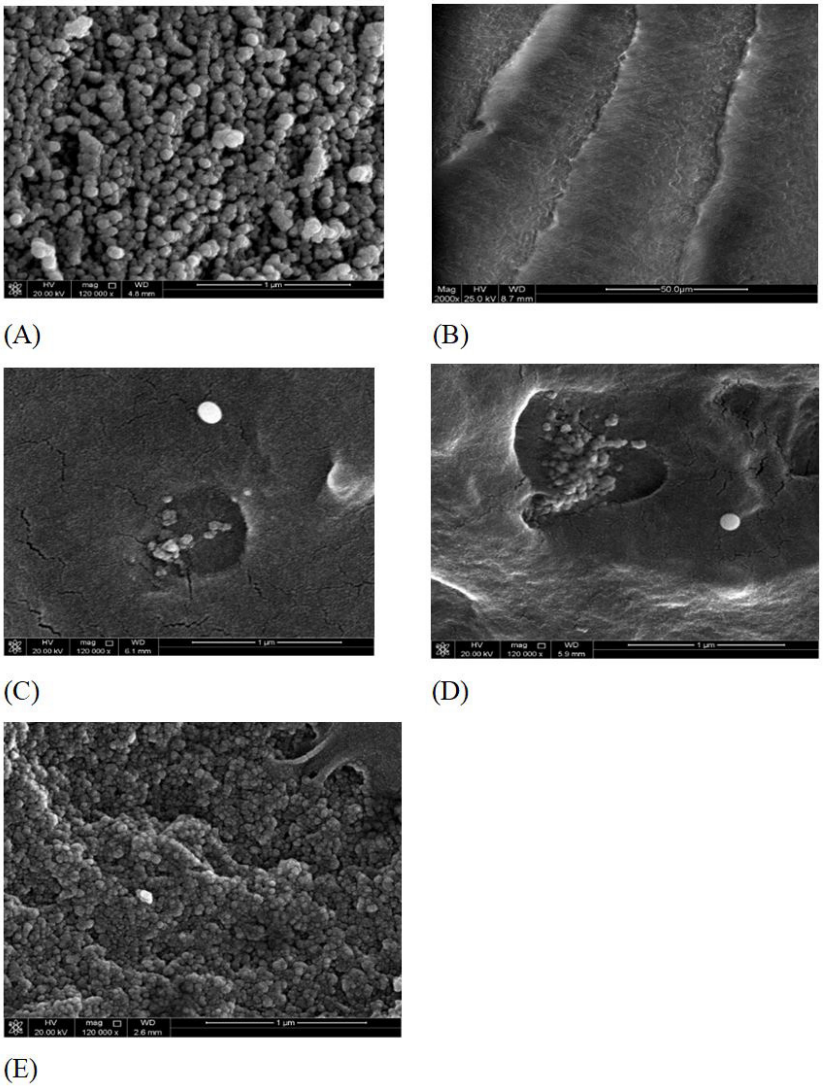

Figure 7: SEM micrographs of the fracture surface of the specimens with different filler contents (A) CB structure, (B) Virgin LLDPE, (C) CB 5wt%, (D) CB 10wt%, (E) CB 20wt%

Rheology Characterization

The rheology characterization of the various composite samples gives an excellent indication of their behavior in an extrusion or a molding process. The rheology also provides a further understanding of the effect of CB on the LLDPE composites. As we can see in Figure 8, the flow behavior of LLDPE is significantly affected by the addition of CB. This is true both at low and high frequencies. The storage modulus of the LLDPE melts (G') increases by about 50 times just by the addition of 5% CB; in the case of 20% CB, it jumps by 130 times. This elastic behavior of the melt is reversed at high frequencies, and the 20% CB composite shows the lowest G' at the highest frequency. This again supports the earlier observation regarding the CB aggregates' agglomeration at the high loading of 20%. The 5% composite is the closest in behavior to the virgin polymer in terms of its melt processing due to the CB particles' good dispersion in the composite matrix. Figure 9 shows the changes in dynamic viscosity as a function of increasing frequency for the different composites. Even though the viscosity of LLDPE is increased by the addition of CB at low shear, this is not the case at high shear rates where the neat polymer maintains a higher viscosity than the composites. CB actually increases the shear thinning of LLDPE as the frequency goes up, as is seen on the right-hand side of Figure 9. Shear-thinning is a known phenomenon in polyethylene [51]. The 5% addition shows the best uniformity and distribution morphology when it comes to the melt processing of LLDPE composites, and the higher loadings of CB significantly change the polymer's processability.

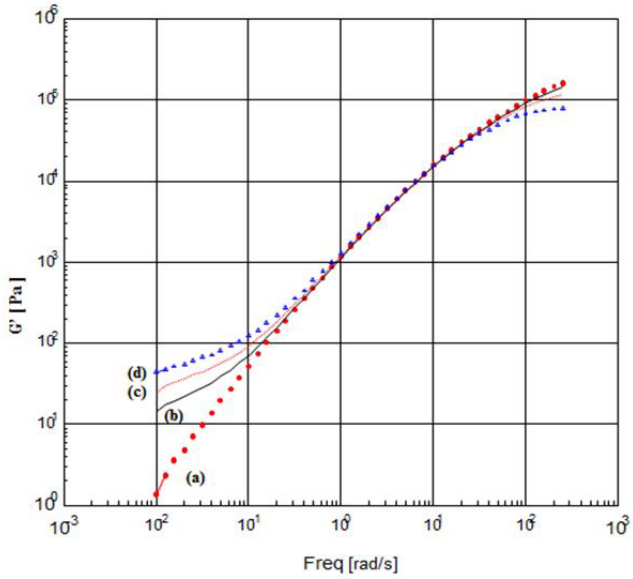

Figure 8: Storage Modulus (G') as a function of frequency for a) virgin LLDPE, b) PE5CB, c) PE10CB, and d) PE20CB

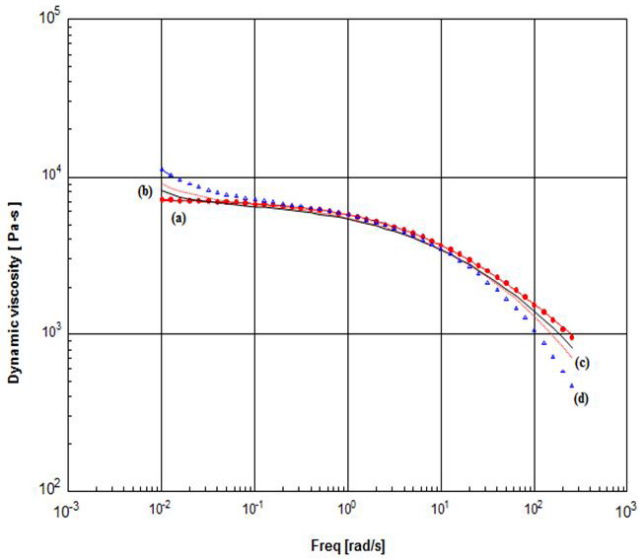

Figure 9: Dynamic Viscosity (η*) as a function of frequency for a) virgin LLDPE, b) PE5CB, c) PE10CB, and d) PE20CB

Electrical Conductivity Measurement

To investigate the effects of the filler and LLDPE content on the conductivity. Figure 10 indicates the reliance of electrical resistivity at room temperature as a comparative carbon black-amount role. As observed, a more outstanding composition of the filled CB particles findings in lower electrical conductivity. The level of diffusion of CB in the 5CB matrix is higher than in the 10CB and 20CB. Here particular, the variation in the polymers' crystallinity performs a leading part in clarifying the resistivity of the CB/thermoplastic polymer compounds explored [52]. The 20 CB has greater resistivity because of its smaller crystallinity. The rising in filler loading more typically has a slight influence on the combined electrical resistivity. The mixture's conductivity falls significantly with the rising quantity of conducting filler in the polymer format, and the combination felt an insulator-to-conductor transition at a specific vital filler substance. This quick breakdown, indicating the accumulation of conducting atoms to shape systems, is well-defined as the percolation transition [13]. In exciting research by Du and coworkers [53], they discovered that the level of alignment necessary to achieve the highest electrical conductivity in the path of nanofiller alignment declines with a rise in nanofiller amounts.

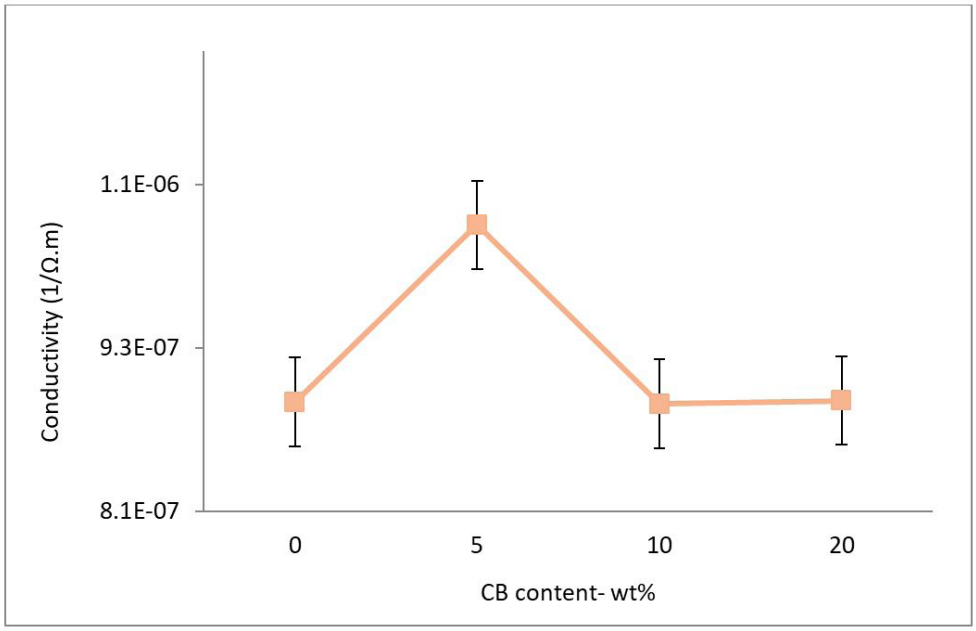

Figure 10: Influence of CB content on conductivity

Conclusion

In this research, composites produced by mixing varying contents of CB nanoparticles and LLDPE were investigated. The findings can be beneficial in the design and operation of LLDPE industrial compounding technology. For thermal analysis of the composites indicated a decrease in the quantity of crystalline phase upon CB's addition. The decrease is significant for PE10CB and PE20CB samples, indicating a lower quantity of the ordered phase with increasing filler content due to agglomeration and limited mobility in the melt during crystallization. The thermal stability is slightly improved for CB-filled LLDPE composites. Carbon black is considered a good conductor; increasing the fillers does not increase the conductivity. The addition of CB to thermoplastics causes a significant increase in viscosity, especially at a low shear rate, where at sufficiently high additives loadings, the viscosity may become unbounded due to strong interaction between the CB particles. It was demonstrated that CB increases the shear-thinning behavior of LLDPE. The overall analysis of thermal, mechanical, and rheology results, leads us to recommend that the optimal loading of CB in the LLDPE composite should be around 5%.

Acknowledgments

The authors would like to thank the support from the Center for Advanced Materials (CAM) at Qatar University and the kind support from Qatar Petrochemical Company (QAPCO). Also want to thank Dr. Noorulnissa Khanim for fruitful discussion. The statements made herein are solely the responsibility of the authors. The authors would like to thank the Central laboratory Unit (CLU), Qatar University, for SEM analysis.

Reference

1. Kato M, Usuki A, Hasegawa N, Okamoto H, Kawasumi M (2011) Development and applications of polyolefin- and rubber-clay nanocomposites. Polym J 43: 583–93.

2. Silva AA, Dahmouche K, Soares BG (2011) Nanostructure and dynamic mechanical properties of silane-functionalized montmorillonite/epoxy nanocomposites. Appl Clay Sci 54: 151–8.

3. Rios P (2015) Preparation of activation. Biomass Chem Eng 2015: 49.

4. Maji PK, Guchhait PK, Bhowmick AK (2009) Effect of nanoclays on physico-mechanical properties and adhesion of polyester-based polyurethane nanocomposites: Structure-property correlations. J Mater Sci 44: 5861–71.

5. Kontou E, Niaounakis M (2005) Thermo-mechanical properties of LLDPE/SiO2 nanocomposites. Polymer (Guildf) 47: 1267–80.

6. Rothon RN (2003) Particulate-Filled Polymer Composites Second Edition. Technology 2003: 544.

7. Deborah DL Chung (1971) Carbon Fiber Composites: 31.

8. Potschke P, Abdel-Goad M, Pegel S, Jehnichen D, Mark JE, et al. (2010) Comparisons among electrical and rheological properties of melt-mixed composites containing various carbon nanostructures. J Macromol Sci Part A Pure Appl Chem 47: 12–9.

9. Pramanik PK, Khastgir D, Saha TN (1992) Conductive nitrile rubber composite containing carbon fillers: Studies on mechanical properties and electrical conductivity. Composites 23: 183–91.

10. Velitchkova K, Krezhov K, Balabanov S (2000) Temperature dependence of surface DC electrical conductivity of carbon-implanted polymers modified by gamma irradiation. Vacuum 58: 531–5.

11. Li Q, Xue QZ, Gao XL, Zheng QB (2009) Temperature dependence of the electrical properties of the carbon nanotube/polymer composites. Express Polym Lett 3: 769–77.

12. Song Y, Zheng Q (2006) Effect of voltage on the conduction of a high-density polyethylene/ carbon black composite at the NTC region. Compos Sci Technol 66: 907–12.

13. Li Q, Siddaramaiah, Kim NH, Yoo GH, Lee JH (2008) Positive temperature coefficient characteristic and structure of graphite nanofibers reinforced high density polyethylene/carbon black nanocomposites. Compos Part B Eng 40: 218–24.

14. El Hasnaoui M, Triki A, Graça MPF, Achour ME, Costa LC, et al. (2012)Electrical conductivity studies on carbon black loaded ethylene butylacrylate polymer composites. J Non Cryst Solids 358: 2810–5.

15. Flandin L, Hiltner A, Baer E (2001) Interrelationships between electrical and mechanical properties of a carbon black-filled ethylene-octene elastomer. Polymer (Guildf) 42: 827–38.

16. Isaji S, Bin Y, Matsuo M (2009) Electrical conductivity and self-temperature-control heating properties of carbon nanotubes filled polyethylene films. Polymer (Guildf) 50: 1046–53.

17. Spitalsky Z, Tasis D, Papagelis K, Galiotis C (2010) Carbon nanotube-polymer composites: Chemistry, processing, mechanical and electrical properties. Prog Polym Sci 35: 357–401.

18. Goldberg VM, Kolesnikova NN, Paverman NG, Kavun SM, Stott PE, et al. (2001) Thermo-oxidative degradation of linear low density poly(ethylene) in the presence of carbon black: A kinetic approach. Polym Degrad Stab 74: 371–85.

19. Liu M, Horrocks AR (2002) Effect of carbon black on UV stability of LLDPE films under artificial weathering conditions. Polym Degrad Stab 75: 485–99.

20. Ahmad A, Mohd DHJ, Abdullah I (2004) Electron beam irradiation of carbon black filled linear low-density polyethylene. J Mater Sci 39: 1459–61.

21. Khan G, Basirun WJ, Kazi SN, Ahmed P, Magaji L, Ahmed SM, et al. (2017) Electrochemical investigation on the corrosion inhibition of mild steel by Quinazoline Schiff base compounds in hydrochloric acid solution. J Colloid Interface Sci 502: 134–45.

22. Almaaded MA, Madi NK, Hodzic A, Soutis C (2014) Influence of additives on recycled polymer blends. J Therm Anal Calorim 115: 811–21.

23. Lee TH, Boey FYC, Khor KA (1995) On the determination of polymer crystallinity for a thermoplastic PPS composite by thermal analysis. Compos Sci Technol 53: 259–74.

24. Quental AC, Felisberti MI (2004) Phase behavior of blends of linear low density polyethylene and poly(ethene-propene-1-butene). Eur Polym J 41: 894–902.

25. Mo S, Chen Y, Jia L, Luo X (2011) Investigation on crystallization of TiO2-water nanofluids and deionized water. Appl Energy 93: 65–70.

26. Nandi S, Ghosh AK (2007) Crystallization kinetics of impact modified polypropylene. J Polym Res 14: 387–96.

27. Luyt AS, Geethamma VG (2006) Effect of oxidized paraffin wax on the thermal and mechanical properties of linear low-density polyethylene-layered silicate nanocomposites. Polym Test 26: 461–70.

28. Yang R, Liu Y, Yu J, Wang K (2006) Thermal oxidation products and kinetics of polyethylene composites. Polym Degrad Stab 91: 1651–7.

29. Ramanaiah K, Ratna Prasad AV, Hema Chandra Reddy K (2011) Mechanical properties and thermal conductivity of typha angustifolia natural fiber-reinforced polyester composites. Int J Polym Anal Charact 16: 496–503.

30. Al-Ali M, Madi NK, Al Thani NJ, El-Muraikhi M, Turos A (2003) Mechanical and thermal properties of gamma-ray irradiated polyethylene blends. Vacuum 70: 227–36.

31. Ling Q, Sun J, Zhao Q, Zhou Q (2011) Effects of carbon black content on microwave absorbing and mechanical properties of linear low-density polyethylene/ethylene-octene copolymer/calcium carbonate composites. Polym - Plast Technol Eng 50: 89–94.

32. AlMaadeed MA, Kahraman R, Noorunnisa Khanam P, Madi N (2012) Date palm wood flour/glass fibre reinforced hybrid composites of recycled polypropylene: Mechanical and thermal properties. Mater Des 42: 289–94.

33. Fan P, Wang L, Yang J, Chen F, Zhong M (2012) Graphene/poly(vinylidene fluoride) composites with high dielectric constant and low percolation threshold. Nanotechnology 2012: 23.

34. Chen L, Gong XL, Li WH (2008) Effect of carbon black on the mechanical performances of magnetorheological elastomers. Polym Test 27: 340–5.

35. AlMaadeed MA, Ouederni M, Noorunnisa Khanam P (2013) Effect of chain structure on the properties of Glass fibre/polyethylene composites. Mater Des 47: 725–30.

36. Marischal L, Cayla A, Lemort G, Campagne C, Éric D (2019) Selection of immiscible polymer blends filled with carbon nanotubes for heating applications. Polymers (Basel) 11: 1–16.

37. Takamura M, Nakamura T, Kawaguchi S, Takahashi T, Koyama K (2010) Molecular characterization and crystallization behavior of peroxide-induced slightly crosslinked poly(L-lactide) during extrusion. Polym J 42: 600–8.

38. Park SJ, Kim HC, Kim HY (2002) Roles of work of adhesion between carbon blacks and thermoplastic polymers on electrical properties of composites. J Colloid Interface Sci 255: 145–9.

39. Zhang Z, Wang C, Zhang J, Mai K (2012) The β-nucleation of polypropylene random copolymer filled by nano-CaCO 3 supported β-nucleating agent. J Therm Anal Calorim 109: 1587–96.

40. Zeng Y, Liu P, Du J, Zhao L, Ajayan PM, Cheng HM (2010) Increasing the electrical conductivity of carbon nanotube/polymer composites by using weak nanotube-polymer interactions. Carbon N Y 48: 3551–8.

41. Kuila T, Bose S, Mishra AK, Khanra P, Kim NH, Lee JH (2012) Effect of functionalized graphene on the physical properties of linear low density polyethylene nanocomposites. Polym Test 31: 31–8.

42. Qiu J, Wu Q, Jin L (2016) Effect of hyperbranched polyethyleneimine grafting functionalization of carbon nanotubes on mechanical, thermal stability and electrical properties of carbon nanotubes/bismaleimide composites. RSC Adv 6: 96245–9.

43. Chipara M, Lozano K, Hernandez A, Chipara M (2008) TGA analysis of polypropylene-carbon nanofibers composites. Polym Degrad Stab 93: 871–6.

44. Chatterjee A, Deopura BL (2006) Thermal stability of polypropylene/carbon nanofiber composite. J Appl Polym Sci 100: 3574–8.

45. Liang JZ, Yang QQ (2009) Mechanical properties of carbon black-filled high-density polyethylene antistatic composites. J Reinf Plast Compos 28: 295–304.

46. Mohamed HFM, Taha HG, Alaa HB (2020) Electrical conductivity and mechanical properties, free volume, and γ-ray transmission of ethylene propylene diene monomer/butadiene rubber composites. Polym Compos 41: 1405–17.

47. Vand AZ (2014) Université De Montréal Development of Polymer Nanocomposite Films and Their Potential for Photovoltaic Cell Applications 2014.

48. Sahoo BP, Naskar K, Tripathy DK (2012) Conductive carbon black-filled ethylene acrylic elastomer vulcanizates: Physico-mechanical, thermal, and electrical properties. J Mater Sci 47: 2421–33.

49. Mostafa A, Abouel-Kasem A, Bayoumi MR, El-Sebaie MG (2008) Insight into the effect of CB loading on tension, compression, hardness and abrasion properties of SBR and NBR filled compounds. Mater Des 30: 1785–91.

50. Chen J, Cui X, Sui K, Zhu Y, Jiang W (2016) Balance the electrical properties and mechanical properties of carbon black filled immiscible polymer blends with a double percolation structure. Compos Sci Technol 140: 99–105.

51. Lin GG, Shih HH, Chai PC, Hsu SJ. Influence of side-chain structures on the viscoelasticity and elongation viscosity of polyethylene melts. Polym Eng Sci 42: 2213–21.

52. Park SJ, Kim JS (2000) Role of chemically modified carbon black surfaces in enhancing interfacial adhesion between carbon black and rubber in a composite system. J Colloid Interface Sci 232: 311–6.

53. Du F, Fischer JE, Winey KI (2005) Effect of nanotube alignment on percolation conductivity in carbon nanotube/polymer composites. Phys Rev B - Condens Matter Mater Phys: 72.